

Providence College

DigitalCommons@Providence

Engineering & Physics Faculty Publications

Engineering & Physics

5-26-2010

Experimental Studies of the NaCs $53\Pi_0$ and $1(a)3\Sigma^+$ States

Seth T. Ashman

Providence College, sashman@providence.edu

Brett McGeehan

Lehigh University

Christopher Wolfe

Lehigh University


Carl Faust

Lehigh University

John Huennekens

Lehigh University

Follow this and additional works at: https://digitalcommons.providence.edu/physics_fac

 Part of the [Atomic, Molecular and Optical Physics Commons](#)

Ashman, Seth T.; McGeehan, Brett; Wolfe, Christopher; Faust, Carl; and Huennekens, John, "Experimental Studies of the NaCs $53\Pi_0$ and $1(a)3\Sigma^+$ States" (2010). *Engineering & Physics Faculty Publications*. 6. https://digitalcommons.providence.edu/physics_fac/6

This Conference Proceeding is brought to you for free and open access by the Engineering & Physics at DigitalCommons@Providence. It has been accepted for inclusion in Engineering & Physics Faculty Publications by an authorized administrator of DigitalCommons@Providence. For more information, please contact dps@providence.edu.

Experimental Studies of the NaCs $5^3\Pi_0$ and $1(a)^3\Sigma^+$ States

S. Ashman, B. M. McGeehan, C. M. Wolfe, C. E. Faust, J. Huennekens
Lehigh University, 16 Memorial Drive East, Bethlehem, PA 18015



Abstract Why Study NaCs?

We present experimental studies of excited electronic states of the NaCs molecule that are currently underway in our laboratory. The optical-optical double resonance method is used to obtain Doppler-free excitation spectra for several excited states. The data that have been identified with the $5^3\Pi_0$ electronic state are used to obtain Rydberg-Klein-Rees (RKR) and Inverse Perturbation Approach (IPA) potential curves for this state. Bound-free spectra from single ro-vibrational levels of electronically excited states to the repulsive wall of the $1(a)^3\Sigma^+$ state also are recorded. Using the previously determined $5^3\Pi_0$ excited state potential, we fit the repulsive wall of the $1(a)^3\Sigma^+$ state to reproduce the experimental spectra using LeRoy's BCONT program. A slightly modified version of BCONT is also being used to fit the relative transition dipole moments, $\mu_e(R)$, as a function of internuclear separation, R, for the various bound-free electronic transitions.

Large permanent dipole moment

Permanent Dipole Moments of Heteronuclear Alkali Molecules in $X^1\Sigma^+$ State

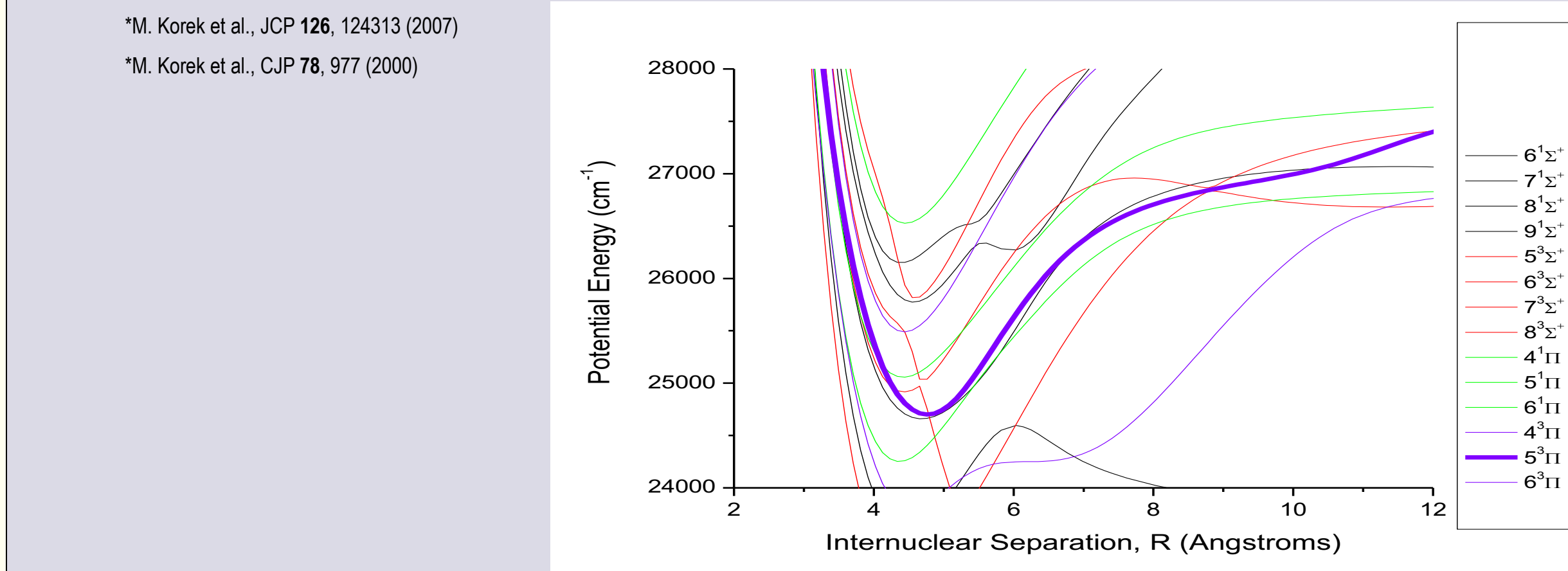
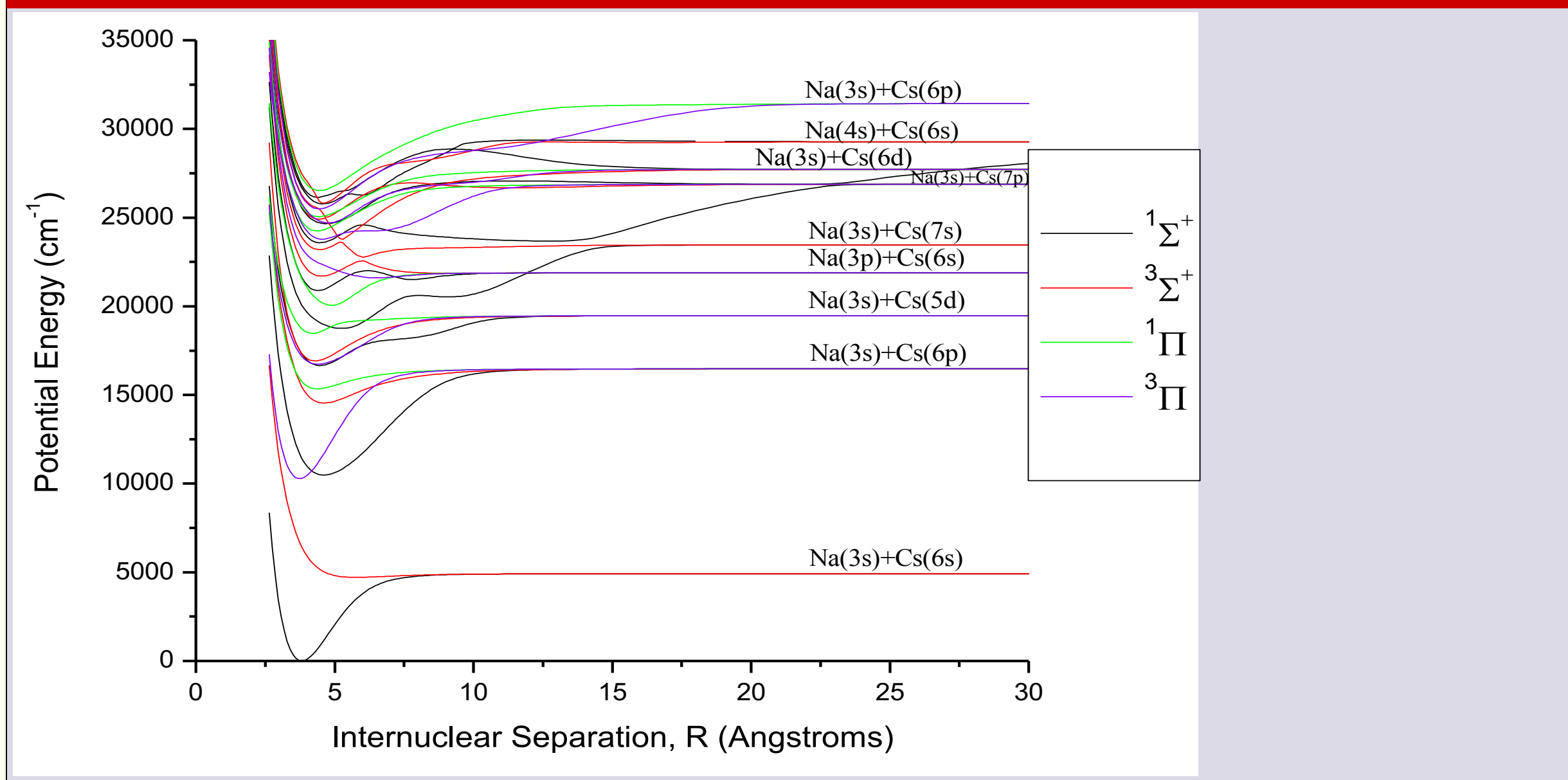
Molecule	Expt. Dipole Moment (Debye)
LiNa	0.47
LiK	3.45
LiRb	4.05
LiCs	6.3
NaK	2.73
NaRb	3.1
NaCs	4.75
KRb	0.2
KCs	2.58
RbCs	2.39

Large spin-orbit interactions:

Spin-Orbit Splitting of Alkali Atoms ($E[P(J=3/2)] - E[P(J=1/2)]$)

Atomic symbol	Splitting (cm^{-1})
Li	0.335
Na	17.196
K	57.71
Rb	273.595
Cs	554.0393
Fr	1686.589

NaCs Theoretical Potentials*



Goals

- Map excited state potentials
- Determine $5^3\Pi_{0=0}$ potential energy curve
- Map repulsive wall of the $a^3\Sigma^+$ state
- Determine transition dipole moment function, $\mu_e(R)$, for transitions between levels of the $5^3\Pi_{0=0}$ and $a^3\Sigma^+$ states
- Study collisional energy transfer
- Study hyperfine structure

Transition Dipole Moment and Selection Rules

Transition Dipole Moment Functions:
Emission intensity for bound-bound or bound-free transitions is proportional to the square of the dipole matrix element

$$I_{\text{emission}} = N_e N_a A_{ul} \quad \text{with} \quad A_{ul} = \frac{8\pi^3 \nu^3}{3c^3} |\mu_{ul}|^2$$

Here, $\mu_{ul} = \int \psi_u^* \hat{\mu} \psi_l d\tau$ where $\hat{\mu} = e \sum_i r_i$ is the dipole operator.

The total wave function can be separated into electronic and nuclear parts, and the nuclear part can be further separated into angular (rotational) and radial (vibrational) terms:

$$\Psi(r, R) = \phi^e(r, R) \psi^v(R) \chi^m(R) \varphi^m(\theta, \phi)$$

(Note that for bound-free transitions, the final state vibrational function must be replaced by a continuum function.)

Thus the dipole matrix element becomes: $\mu_{ul} = \int \psi_u^* \hat{\mu} \psi_l d\tau = \int \phi_u^* \phi_l d\tau \int \psi_u^* \psi_l dR \int \varphi_u^* \varphi_l d\Omega$

For a transition between two electronic states, initial state u and final state l , the nuclear term is zero, the angular terms of the ϕ_u integral lead to selection rules on J , and the radial term leads to $\mu_{ul} \propto \int \chi_u^m(R) \chi_l^m(R) dR$ with $\mu_{ul}(R) = \int \phi_u^*(r, R) \hat{\mu} \phi_l(r, R) d\tau$

Therefore, $\mu_{ul}(R)$ can be obtained by fitting the intensities of bound-bound emission lines or bound-free emission continua to experimental spectra.

Selection Rules for Electronic Transitions

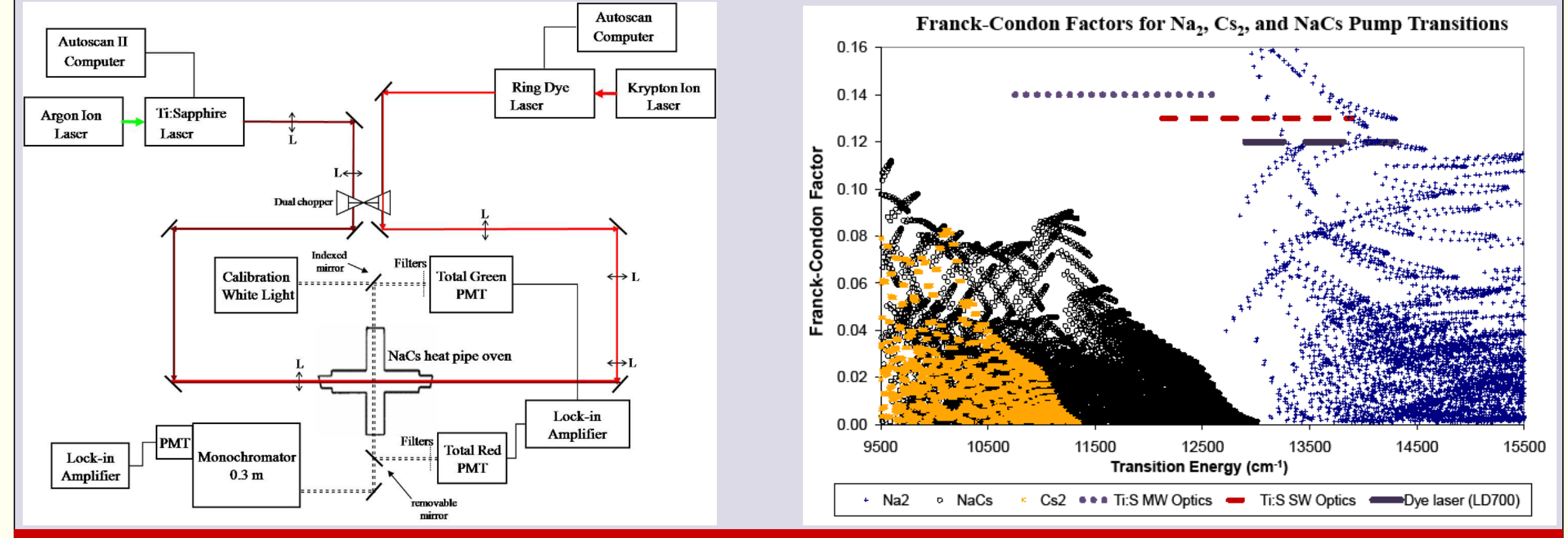
$\Delta \Omega = \text{anything}$

$\Delta J = 0, \pm 1$ with restriction that $\Delta J = 0$ forbidden for $\Sigma \leftrightarrow \Sigma$ transitions

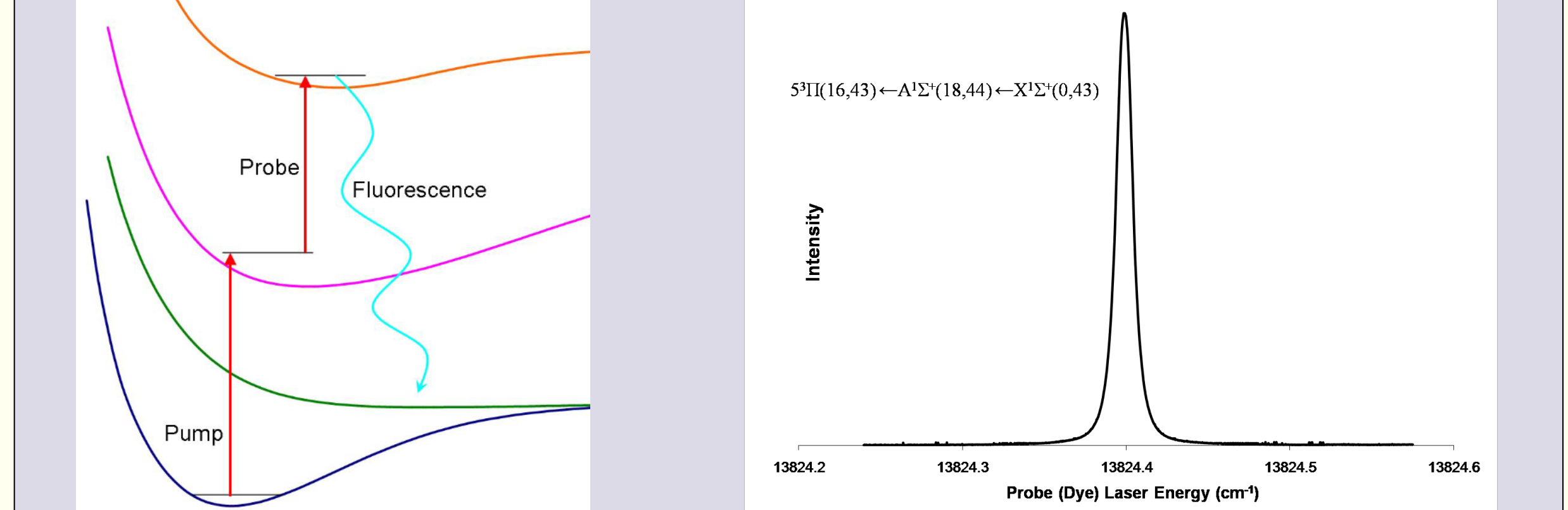
Hund's case a)
 $\Delta S = 0$
 $\Delta \Lambda = 0, \pm 1$
 $\Delta \Omega = 0, \pm 1$

Hund's case c)
 $\Delta \Omega = 0, \pm 1$

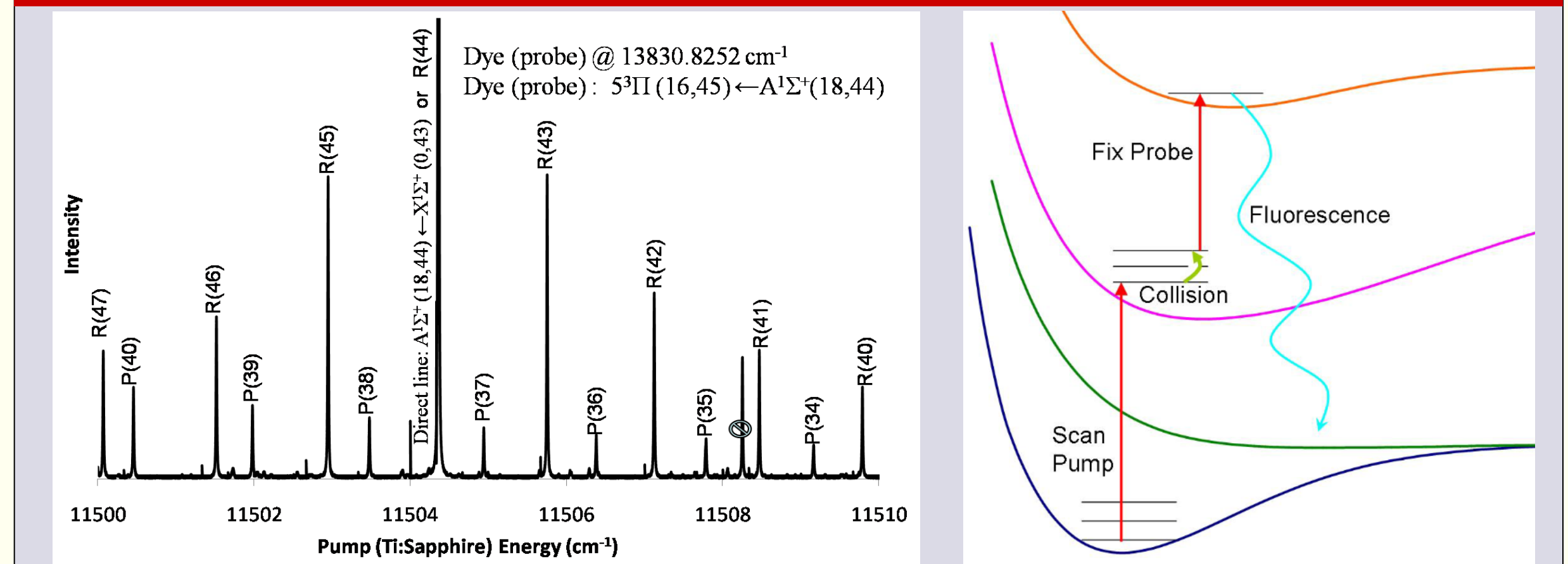
Experimental Setup Franck-Condon Factors $A^1\Sigma^+ \leftarrow X^1\Sigma^+$



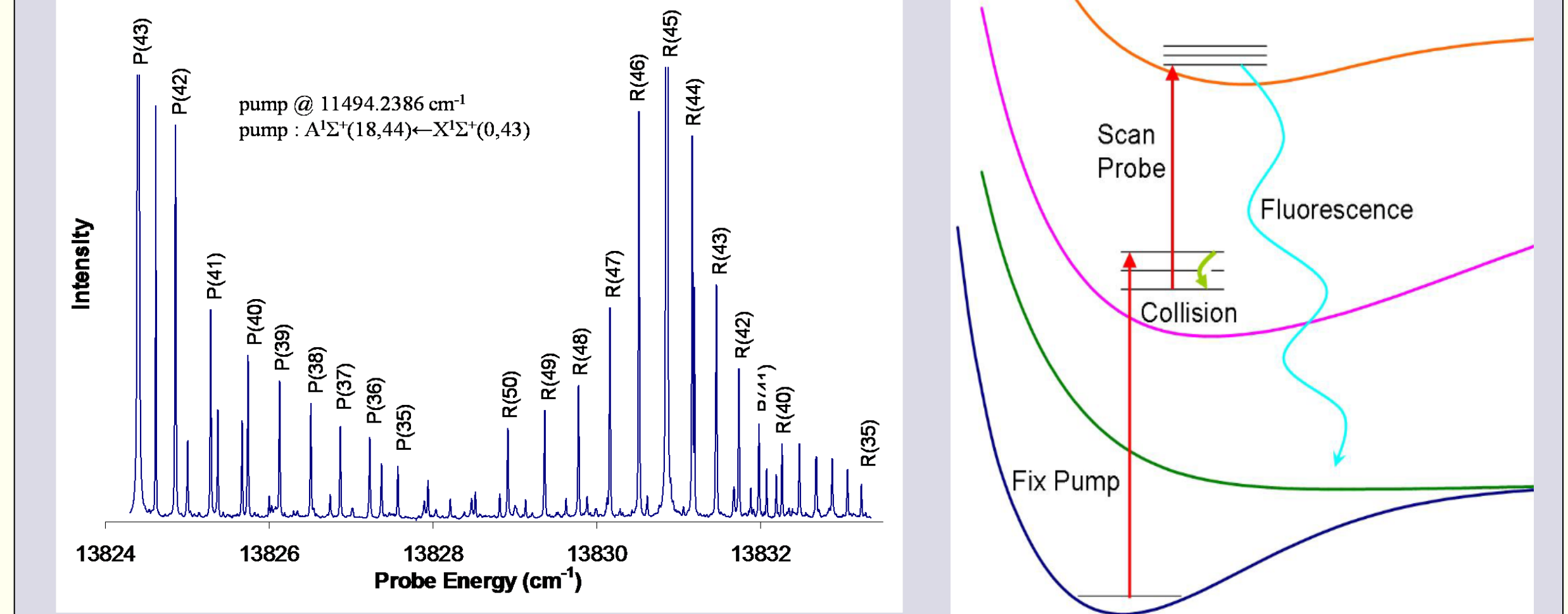
Double Resonance Excitation



Collisional Population Transfer

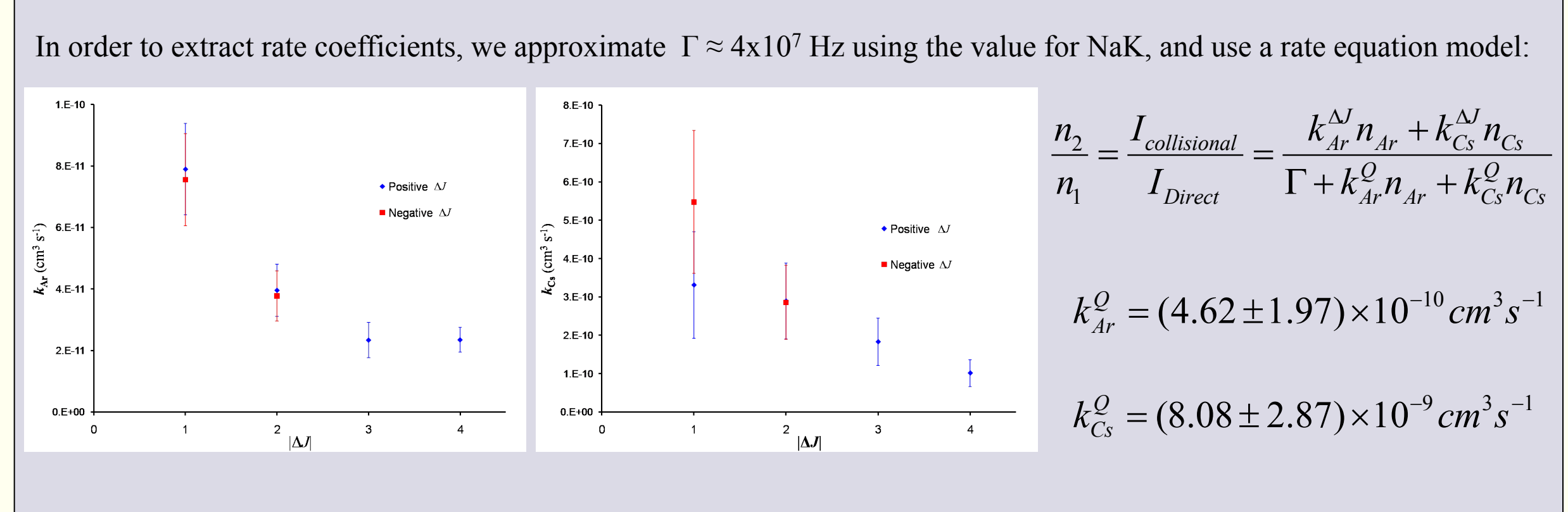
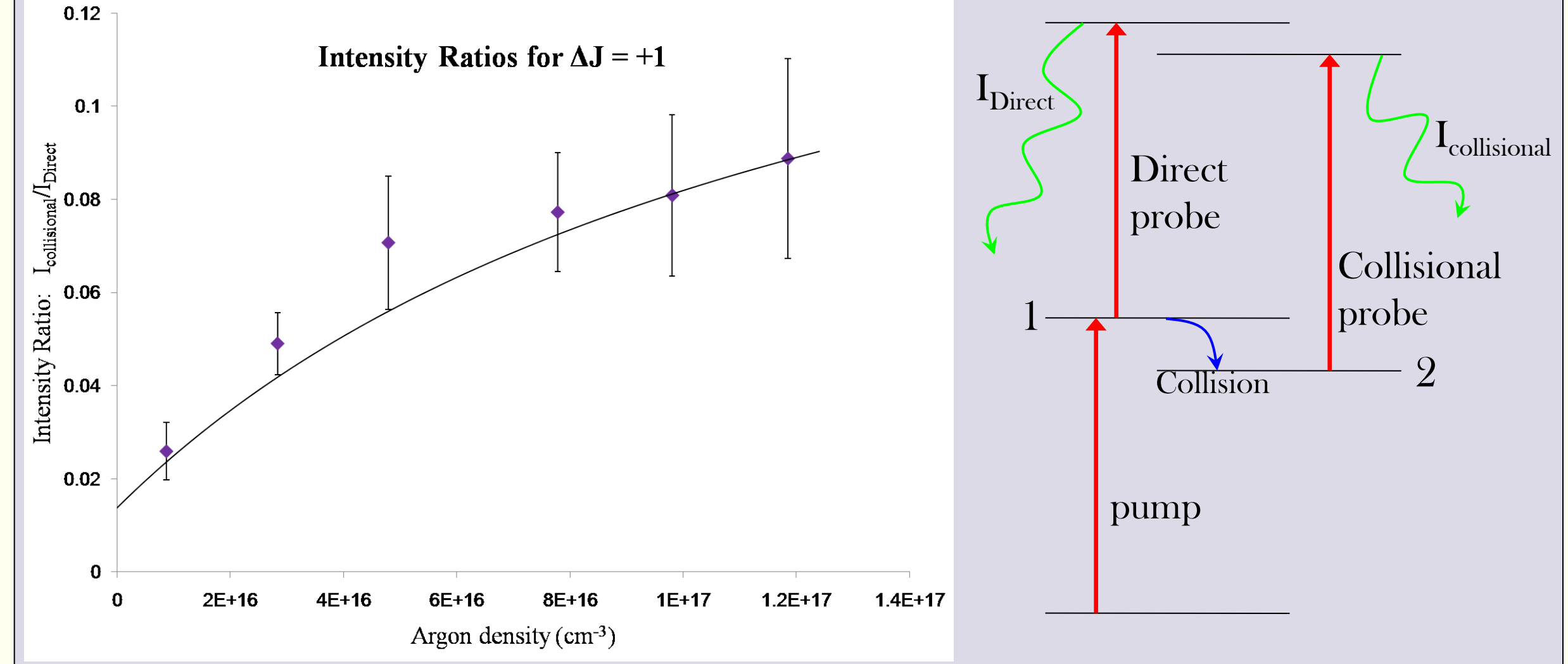


• Fixing the probe and scanning the pump allows the intermediate state levels to be labeled. Collisional satellite lines allow intermediate state $[A^1\Sigma^+(v', J)]$ level energies for a large number of rotational levels to be determined relative to known ground state levels $[X^1\Sigma^+(v'', J'']$.

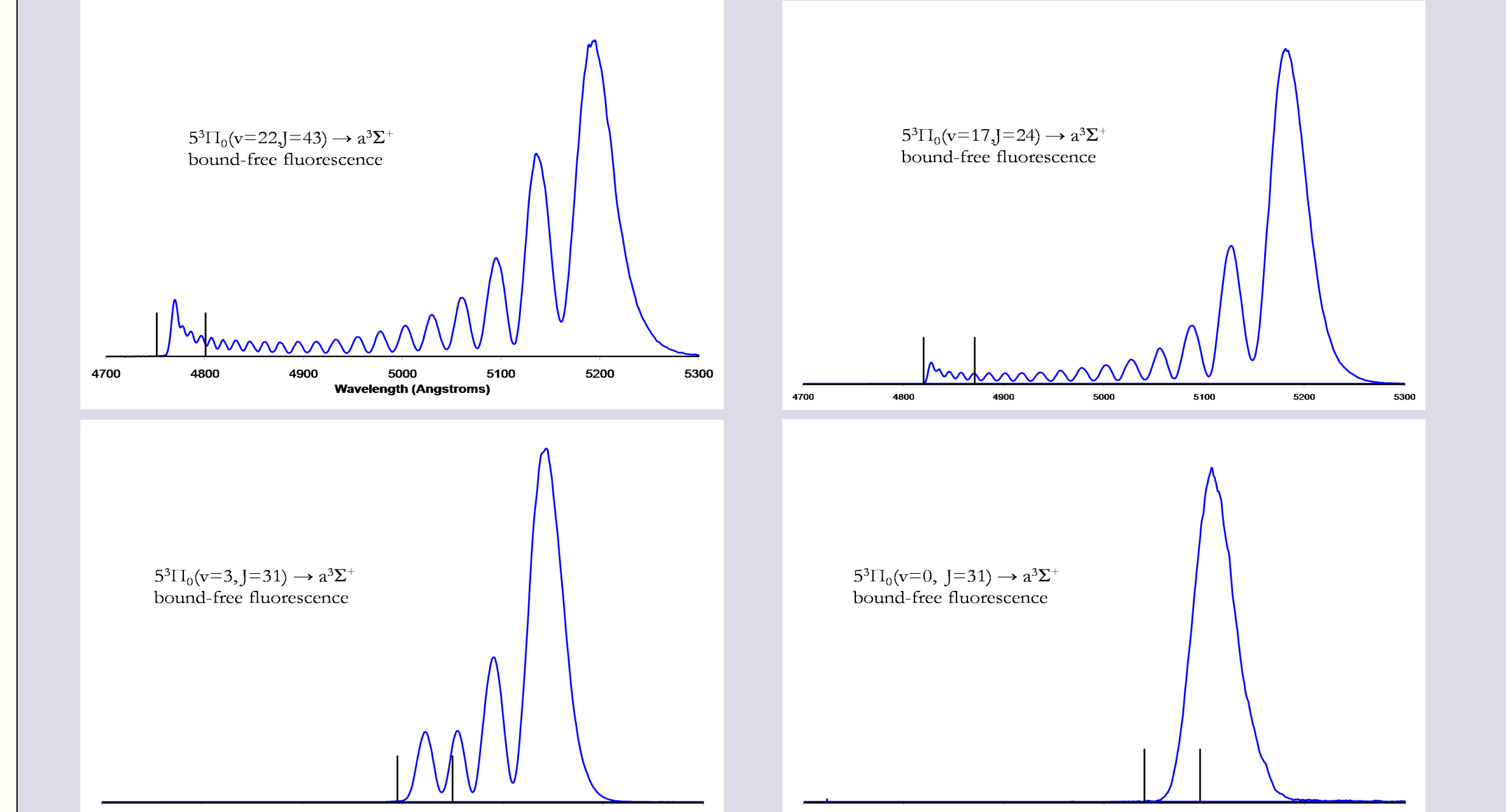


• Then fixing the pump and scanning the probe allows the excited state levels to be labeled. Again collisional satellite lines allow the upper state level energies for a large number of rotational levels to be accurately determined relative to $A^1\Sigma^+(v', J')$ levels.

Collision Rates

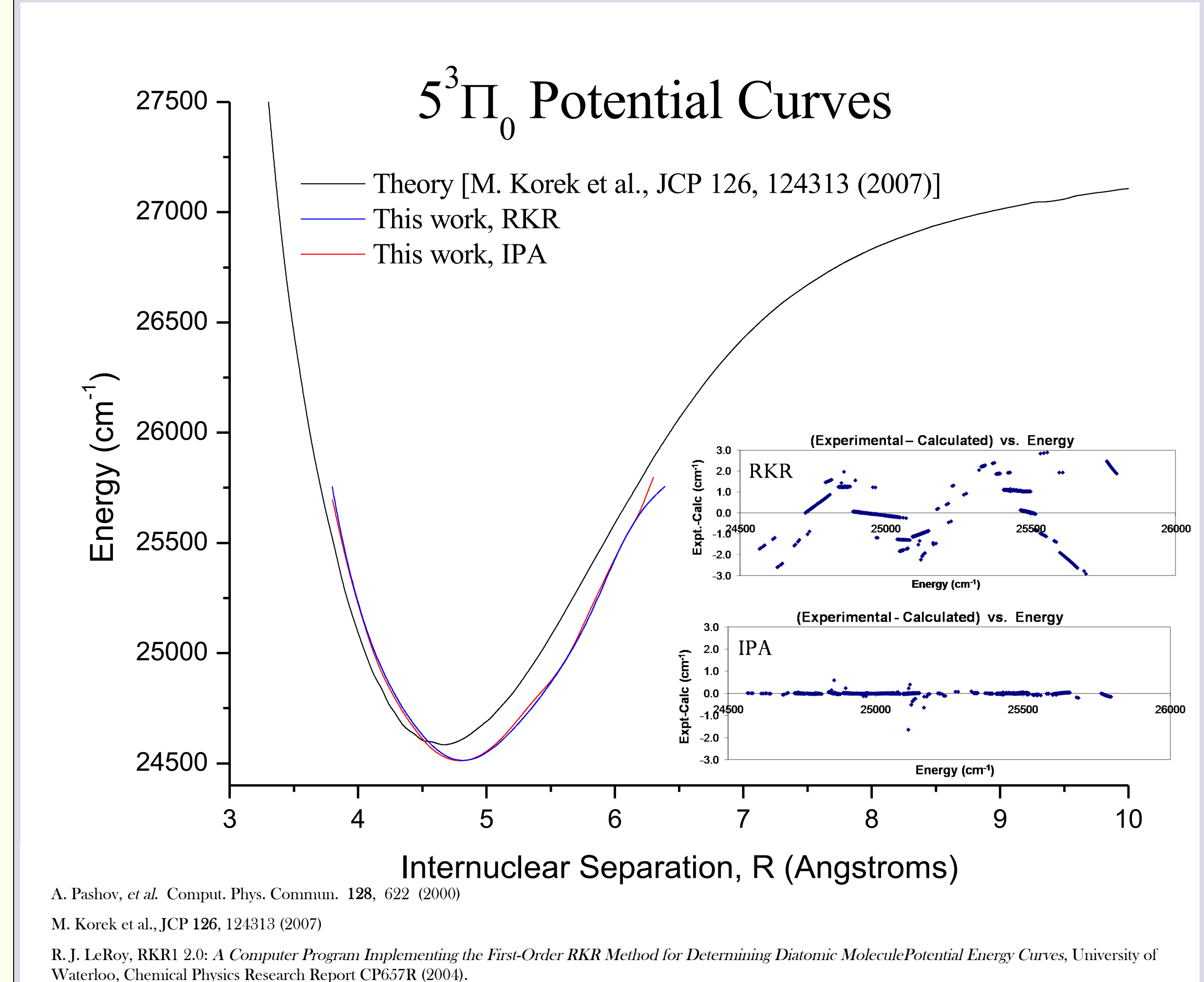


Resolved $5^3\Pi_0$ Fluorescence Spectra



The black vertical lines in each scan denote the difference in energy between the selected $5^3\Pi_0$ level to the $a^3\Sigma^+$ asymptotic limit or to the bottom of its shallow well. Thus the parts of the spectra between the vertical lines represents unresolved bound-bound transitions. A monotonic difference potential produces simple reflection spectra, which provide an easy method to determine the upper state vibrational quantum number at small values of v .

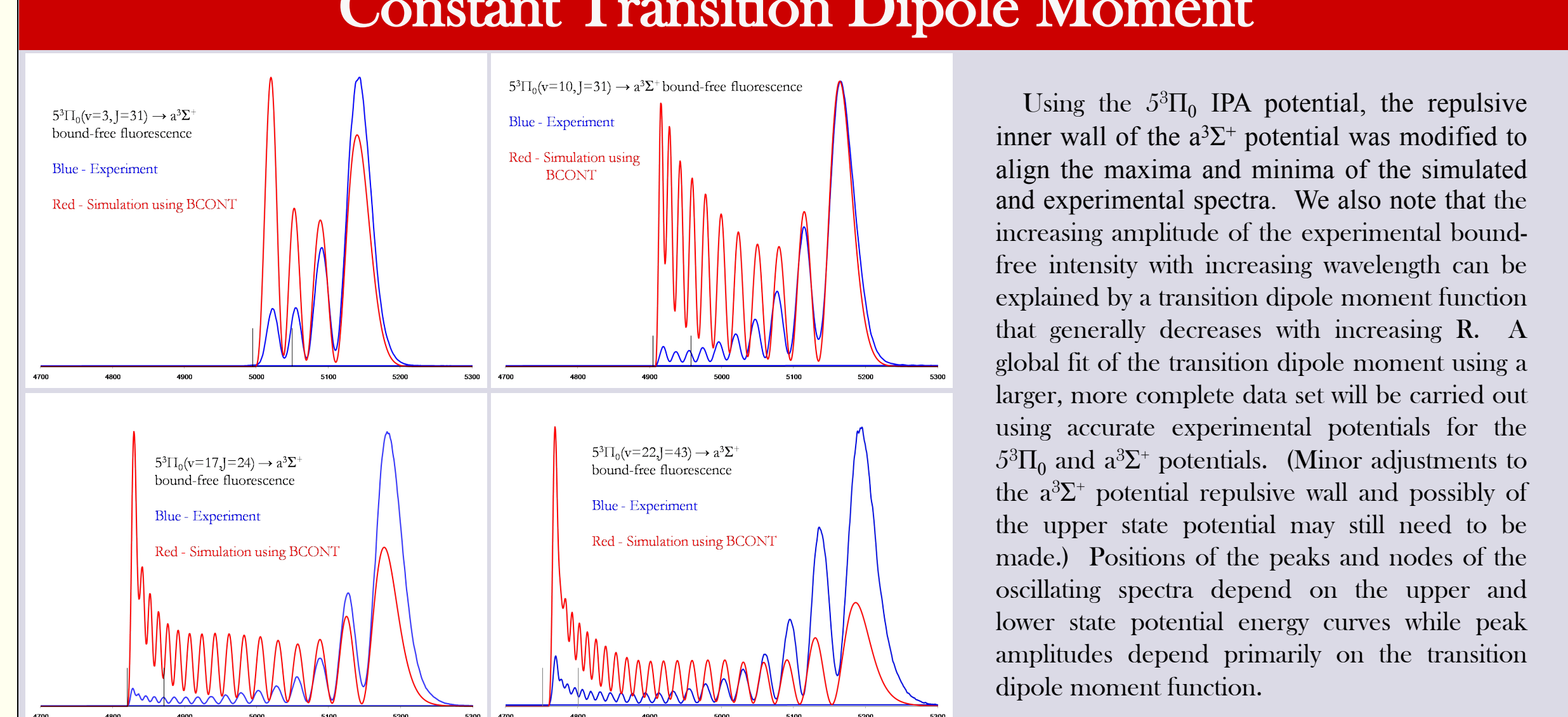
$5^3\Pi_0$ Theoretical, RKR, and IPA Potentials



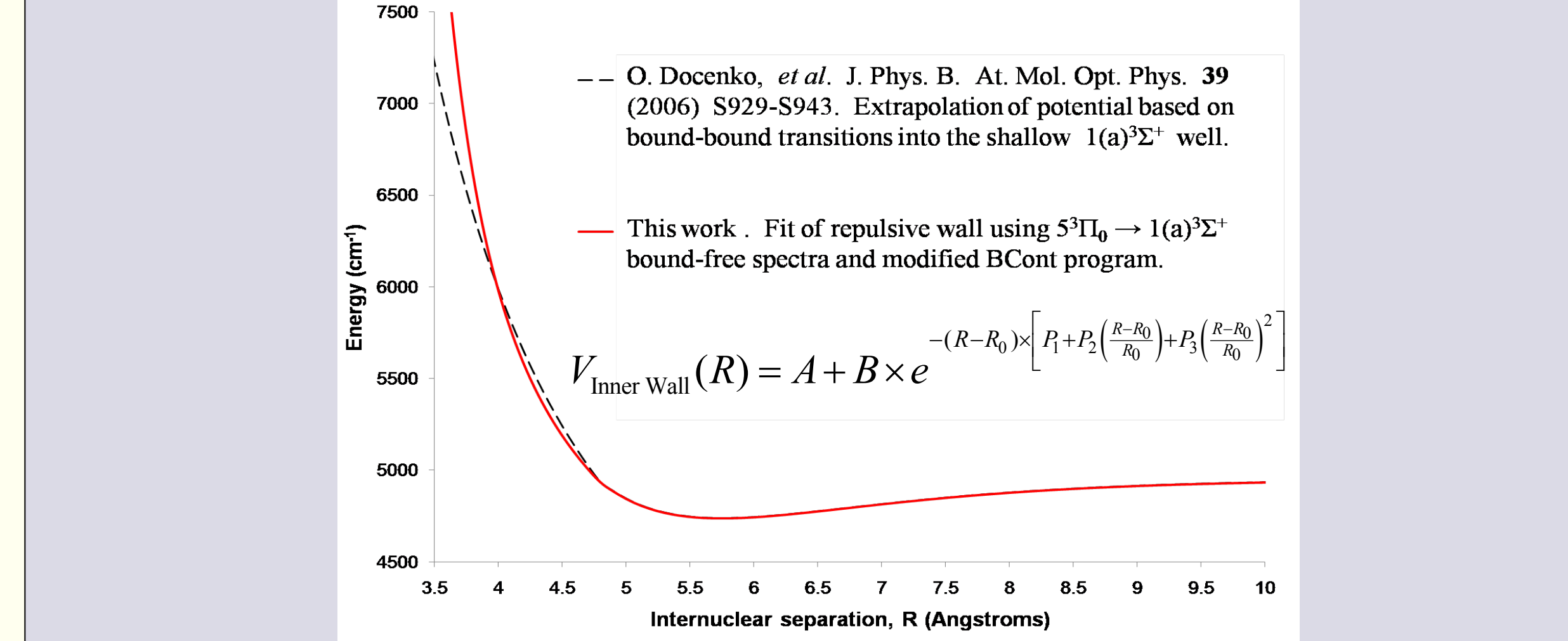
Dunham Coefficients for $5^3\Pi_0$ State

Parameter	Energy* ± Error** (cm^{-1})	Theoretical values*** (cm^{-1})
Te	24511.79 ± 0.89	24880
Y(1,0)	64.24 ± 0.43	58.6
Y(2,0)	-1.750 ± 0.068	-
Y(3,0)	0.1060 ± 0.0041	-
Y(4,0)	-(2.211 ± 0.085) × 10 ⁻³	-
Y(0,1)	0.03706 ± 0.00018	0.0394
Y(1,1)	-(4.0 ± 1.6) × 10 ⁻⁵	-
Y(0,2)	-7.2 × 10 ⁻⁸ (fixed in fit)	-

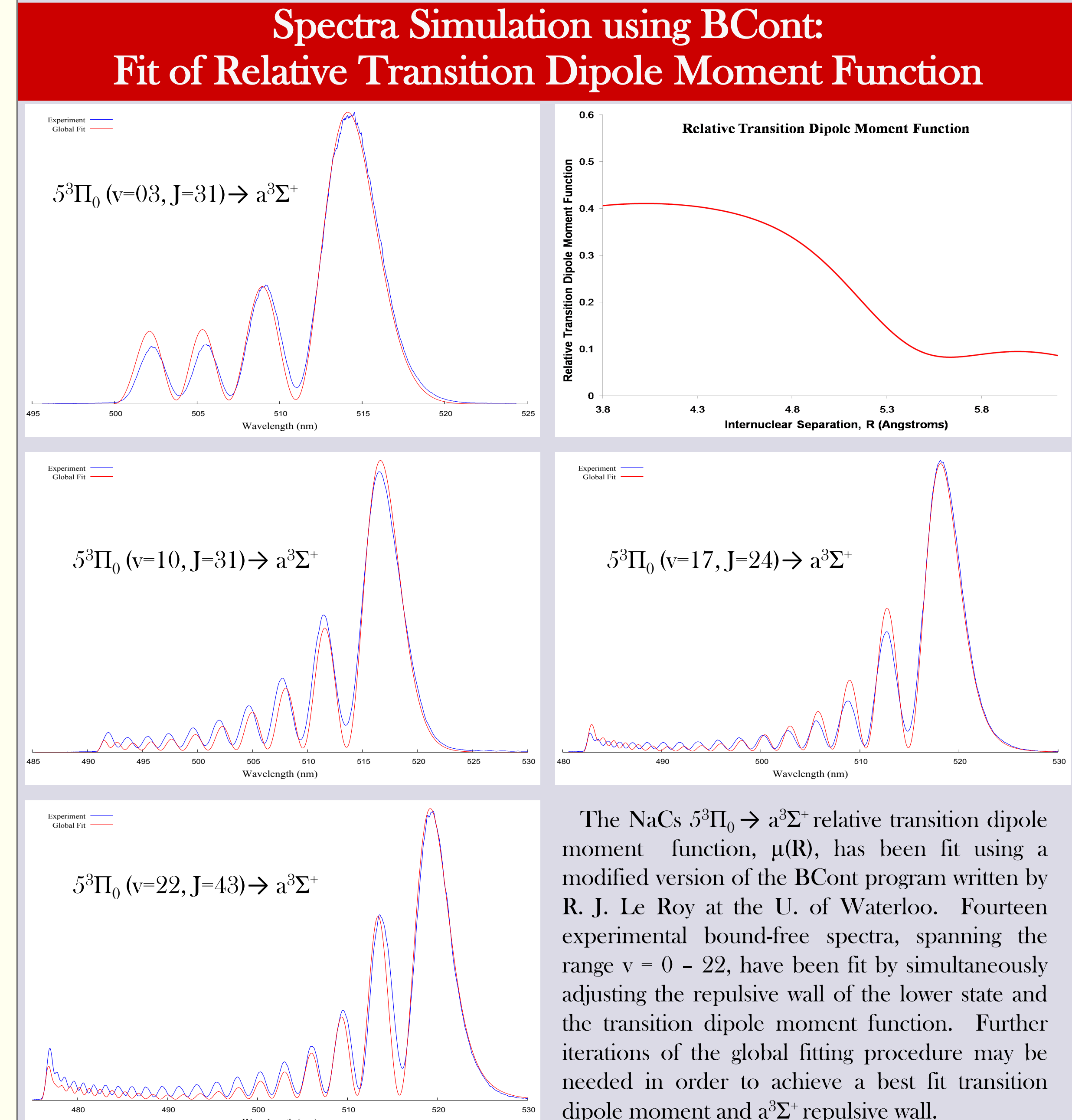
Spectra Simulation using BCont: Constant Transition Dipole Moment



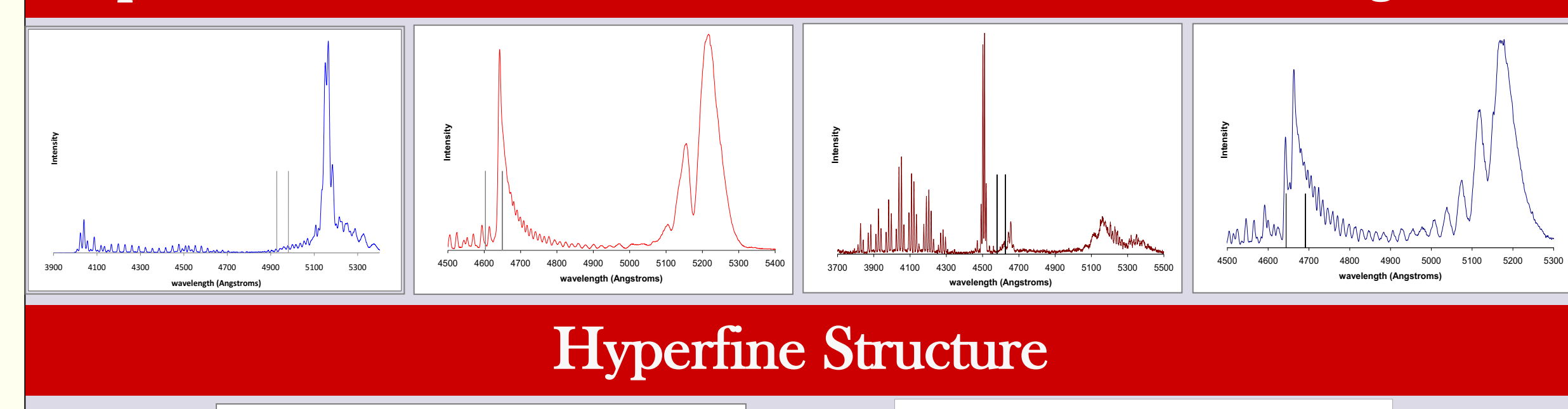
Modified $a^3\Sigma^+$ Repulsive Wall



Spectra Simulation using BCont: Fit of Relative Transition Dipole Moment Function



Spectra of Other NaCs Excited States Under Investigation



Hyperfine Structure

NaK $3^3\Pi$ hyperfine

Previous work on NaK showed a rich variety of hyperfine structure. Ongoing studies of NaCs have yet to reveal clear hyperfine structure. Hyperfine interaction in NaCs should be described by:

$$E_{\text{hfs}} = b_{\Sigma} \mathbf{I} \cdot \mathbf{S} + b_{\Sigma}^{\Omega} K J(J+1) - S(S+1) - N(N+1)$$

From this we expect a larger hyperfine interaction for NaCs. However, states of NaK can often be described by Hund's case b_{Σ} or b_{Σ}^{Ω} , while NaCs has a much stronger spin-orbit interaction and is likely described by Hund's case c.

Hund's case b_{Σ}
 $E_{\text{hfs}}^c \approx \frac{b_{\Sigma} K J(J+1) - S(S+1) - N(N+1)}{4 J(J+1)}$

Hund's case c
 $E_{\text{hfs}}^c \approx \frac{b_{\Sigma} K}{2} \frac{\Sigma \Omega}{J(J+1)}$

Hund's Coupling Case (c)
 $\Delta E_{\text{hfs}}^c \propto b_{\Sigma} I \cdot J$

Therefore, the hyperfine structure might only be observable at lower J values for states with non-zero values of Σ and Ω .